

COMBUSTION INSTABILITY WITH FINITE MACH

NUMBER FLOW AND ACOUSTIC LINERS

by Richard J. Priem and Edward J. Rice

Lewis Research Center
Cleveland, Ohio

TECHNICAL PAPER proposed for presentation at

Twelfth International Symposium on Combustion
sponsored by the Combustion Institute
Poitiers, France, July 14-20, 1968

NATIONAL AERONAUTICS AND SPACE ADMINISTRATION

COMBUSTION INSTABILITY WITH FINITE MACH

NUMBER FLOW AND ACOUSTIC LINERS

by Richard J. Priem and Edward J. Rice

Lewis Research Center
National Aeronautics and Space Administration
Cleveland, Ohio

SUMMARY

Combustion instability phenomena are examined theoretically using a small amplitude, linear analysis. Conservation equations are solved for finite axial gas velocities in the combustion chamber. Transverse waves with axial variations were considered. Concentrated combustion near the injector face was assumed. The general wave equations are solved for specific boundary conditions at the end of the chamber (nozzle entrance), walls of the chamber (acoustic liners) and the injector (combustion zone).

Calculated curves are presented to illustrate how Mach number, chamber length to radius ratio, nozzle flow response, and acoustic liners influence the combustion response required to obtain neutral stability or various growth rates. These curves demonstrate the importance of the perturbations in combustion rate that are 90° out of phase with the pressure perturbations. The variations in pressure amplitude and phase, or time displacement, with axial position are presented to illustrate how the combustion process can influence the

wave characteristics. For example, it is shown that a combustor can have oscillations over a range of frequencies that are dependent on the combustion process.

Results of stability tests with a 20 000-pound thrust hydrogen-oxygen combustor are briefly analyzed with the aid of the calculated neutral stability limits. The comparison illustrates how the combustion response calculations can be used to predict stability or what acoustic liner is required to stabilize a combustor.

INTRODUCTION

Recent combustion instability experience has demonstrated several interesting phenomena that have not been described theoretically. Most interesting of these is that acoustic absorbing chamber walls change stability limits and frequencies of the instability (see ref. 1). Detailed pressure measurements have shown (refs. 2 and 7) that waves travel as transverse acoustic waves but they do not have constant amplitude and phase with length. Other data indicate that the frequencies of the instability do not always correspond to those calculated for pure acoustic modes. These theoretically unexplained results motivated this study.

The variations in the transverse wave properties with length suggest that modifying the theoretical approach of ref. 3 to include axial variations would be successful. The data with acoustic liners

indicated that the boundary conditions at the walls would be controlled by the liner. Therefore various boundary conditions would have to be included in the theory. Recent publications (refs. 4 and 5) wherein the combustion process is characterized by a response function (perturbation in burning produced by a perturbation in pressure) suggest that a term like a response function be used to generally characterize the combustion process. Since most combustors operate at high gas velocities or Mach numbers within the chamber it also seemed necessary to allow for high Mach numbers.

All of these aspects were incorporated in a theory to obtain a relatively simple equation to characterize the stability characteristics of a system. Calculations were then performed to illustrate how various design parameters influence the stability characteristics. Experimental stability characteristics of a 20 000-pound thrust hydrogen oxygen combustor are compared to the calculated results to illustrate how to use the theoretical results and the validity of the theory.

THEORY

For this analysis it is assumed that combustion is concentrated in a zone immediately adjacent to the injector face. It is also assumed that during unsteady operation, small amplitude, three-dimensional, irrotational waves propagate through the chamber. These waves must satisfy the boundary conditions of the chamber. The waves produce

a perturbation in the combustion rate at the injector face which is determined by the impedance of the combustion process. The waves also produce a perturbation in flow at the end of the cylindrical chamber, or entrance to the convergent nozzle, which is determined by the impedance of the nozzle. Similarly, if the walls of the cylindrical chamber have acoustic absorbing characteristics, the waves will produce a perturbation in velocity at the wall which is also determined by an impedance.

The equations of motion of an inviscid compressible fluid, which describe the waves in the chamber can be written in nondimensional form (ρ , P and T are nondimensionalized by their average values, velocity by speed of sound, coordinates by R and time by $2R/0.586 a$)

$$\begin{array}{ll}
 \rho_t + \nabla \cdot (\rho u) = 0 & \text{Cont.} \\
 \rho \frac{Du}{Dt} + \frac{1}{\gamma} \nabla P = 0 & \text{Mom.} \\
 \rho \frac{DT}{Dt} - \frac{\gamma - 1}{\gamma} \frac{DP}{Dt} = 0 & \text{Energy} \\
 P = \rho T & \text{State}
 \end{array} \quad \left. \vphantom{\begin{array}{l} \text{Cont.} \\ \text{Mom.} \\ \text{Energy} \\ \text{State} \end{array}} \right\} \quad (1)$$

Defining a velocity potential Φ such that $\nabla\Phi = u$ then eq. (1) yields (see ref. 3)

$$\left. \begin{aligned}
 Q \nabla^2 \Phi - \Phi_{tt} &= 2 \nabla \Phi \cdot \nabla \Phi_t + \frac{\gamma - 1}{2} (\nabla \Phi \cdot \nabla \Phi) \nabla^2 \Phi \\
 &+ \frac{1}{2} \nabla \Phi \cdot \nabla (\nabla \Phi \cdot \nabla \Phi) + (\gamma - 1) \Phi_t \nabla^2 \Phi \\
 Q - P^{(\gamma-1)/\gamma} &= (\gamma - 1) \left[\Phi_t + \frac{1}{2} \nabla \Phi \cdot \nabla \Phi \right]
 \end{aligned} \right\} \quad (2)$$

Now Φ and P can be expanded in a series in powers of some amplitude parameter ϵ . Thus

$$\left. \begin{aligned}
 \Phi &= \Phi^{(0)} + \epsilon \Phi^{(1)} + \epsilon^2 \Phi^{(2)} + \dots \\
 P &= 1 + \epsilon P^{(1)} + \epsilon^2 P^{(2)} + \dots
 \end{aligned} \right\} \quad (3)$$

Since $\nabla \Phi^{(0)} = M$ then eq. (2) yields the following terms containing ϵ to the first order.

$$-\Phi_{tt}^{(1)} + \nabla^2 \Phi^{(1)} = M^2 \frac{\partial^2 \Phi^{(1)}}{\partial Z^2} + 2M \frac{\partial \Phi_t^{(1)}}{\partial Z}$$

$$P^{(1)} = -\gamma \Phi_t^{(1)} - \gamma M \frac{\partial \Phi^{(1)}}{\partial Z} \quad (4)$$

If it is assumed that the solution of equation(4) is periodic in time and separable in the Z -, r -, and θ -coordinates the following solutions are obtainable.

$$\Phi^{(1)} = J_n(mr) e^{in\theta} e^{i\omega t} \left(e^{izB_1} + C e^{izB_2} \right) \quad (5)$$

where

$$B_1 = \frac{\omega M + \sqrt{\omega^2 M^2 + (M^2 - 1)(m^2 - \omega^2)}}{1 - M^2} \quad (6)$$

$$B_2 = \frac{\omega M - \sqrt{\omega^2 M^2 + (M^2 - 1)(m^2 - \omega^2)}}{1 - M^2}$$

and

$$P^{(1)} = -i\gamma \left[J_n(mr) e^{in\theta} e^{i\omega t} \right] \left[\begin{aligned} &\omega \left(e^{izB_1} + C e^{izB_2} \right) \\ &+ n \left(B_1 e^{izB_1} + B_2 C e^{izB_2} \right) \end{aligned} \right] \quad (7)$$

$$v_z^{(1)} = iJ_n(mr) e^{in\theta} e^{i\omega t} \left(B_1 e^{izB_1} + B_2 C e^{izB_2} \right) \quad (8)$$

$$v_r^{(1)} = \left[\frac{n}{r} J_n(mr) - m J_{n+1}(mr) \right] e^{in\theta} e^{i\omega t} \left(e^{izB_1} + C e^{izB_2} \right) \quad (9)$$

$$v_\theta^{(1)} = inJ_n(mr) e^{in\theta} e^{i\omega t} \left(e^{izB_1} + C e^{izB_2} \right) \quad (10)$$

In eqs. (5) to (10), the terms n , m , ω , B_1 , B_2 , and C carry the following connotation.

- n number of waves that exist in the θ direction and must be an integer
- ω complex number, the real part specifying the frequency of the oscillation and the imaginary portion specifies the growth or decay rate with time

- m complex eigenvalue of the radial differential equation as determined by the wall boundary conditions
- B_1, B_2 complex numbers whose real values specify the speed at which a wave travels axially up or down the chamber. The imaginary part specifies the decay in amplitude with length
- C complex number which characterizes the waves at the nozzle end of the chamber

A flow response is assumed to characterize the boundary conditions at the nozzle and injector and a velocity response at the wall as given by:

$$G \equiv \frac{W^{(1)}}{P^{(1)}} = \frac{\rho^{(1)}MA + v_z^{(1)}A}{MAP^{(1)}} = \frac{1}{\gamma} + \frac{v_z^{(1)}}{MP^{(1)}} \Bigg|_{z=\text{nozzle}} \quad (11)$$

$$N \equiv \frac{W^{(1)}}{P^{(1)}} = \frac{1}{\gamma} + \frac{v_z^{(1)}}{MP^{(1)}} \Bigg|_{z=\text{injector}} \quad (12)$$

$$K \equiv \frac{P^{(1)}g}{v_r^{(1)} a \frac{2}{\rho}} = \frac{P^{(1)}}{\gamma v_r^{(1)}} \Bigg|_{r=\text{wall}}$$

Substituting eqs. (7) and (8) in eq. (11) to determine the nozzle response at the nozzle end of the chamber ($Z = 0$) and solving for C:

$$C = - \left[\frac{B_1(1 - M + \gamma GM^2) + \omega(\gamma G - 1)M}{B_2(1 - M + \gamma GM^2) + \omega(\gamma G - 1)M} \right] \quad (13)$$

Substituting eqs. (7) and (8) in eq. (11) to determine the combustion response N at the injector end of the chamber ($Z = -L$):

$$N = \text{Re}(N) + i\text{Im}(N) = \frac{1}{2} \left\{ 1 - \frac{(B_1 e^{-iLB_1} + B_2 C e^{-iLB_2})}{M[\omega(e^{-iLB_1} + C e^{-iLB_2}) + M(B_1 e^{-iLB_1} + B_2 C e^{-iLB_2})]} \right\} \quad (14)$$

Substituting eqs. (7) and (9) in eq. (12) to determine the wall response K at the chamber wall ($r = 1$):

$$K = \text{Re}(K) + i\text{Im}(K) = \frac{-iJ_n(m) \left[(e^{izB_1} + C e^{izB_2}) + M(B_1 e^{izB_1} + B_2 C e^{izB_2}) \right]}{\left[nJ_n(m) - mJ_{n+1}(m) \right] \left(e^{izB_1} + C e^{izB_2} \right)} \quad (15)$$

The amplitude (P_{\max}) of the wave, determined from the product of the pressure and its complex conjugate, and the angular position (β) of maximum amplitude at any time, and radial or axial position is given by:

$$P_{\max}^2 = P_a \times P_a^* \tag{16}$$

$$\tan \beta = -\frac{\text{Im}(P_a)}{\text{Re}(P_a)}$$

where

$$P_a = -i\gamma J_n(mr)e^{i\omega t} \left[\omega(e^{iB_1z} + e^{iB_2z}) + M(B_1e^{iB_1z} + B_2Ce^{iB_2z}) \right]$$

Equations (6), (13), (14), and (15) were solved on an IBM 7094 computer for various values ω , m , M , L/R , and G and for $n = 1$ (first transverse mode) to obtain combustion responses (N) and wall responses (K). For hard walls or $K \approx \alpha$, a value of m of 1.84118 is used. For soft wall ($K \neq \alpha$), since K varies with chamber length, a trial and error technique was used to determine which value of m produced the desired average value of K over the full chamber length. Pressure profiles were determined from equations (6), (13) and (16) to determine maximum amplitude and phase of the wave relative to the injector end of the chamber as a function of length.

RESULTS AND DISCUSSION

Stability calculations were performed to examine and illustrate the influence of various parameters (i. e., decay coefficient, length to radius ratio, Mach number, nozzle response and wall response) on stability and wave characteristics. A combustor with $L/R = 2.7$,

Mach number = 0.33, nozzle impedance of $\text{Re}(G) = 0.9166$ and infinite wall impedance was used as a reference condition (to illustrate how varying one parameter at a time from the reference combustor changed the stability and wave characteristic). The reference combustor conditions were selected to match those of a 20 000-pound thrust hydrogen oxygen engine extensively tested at the Lewis Research Center (ref. 6).

Stability lines for various growth or decay coefficients are shown in figure 1. The neutral stability line (waves will not grow or decay) shows that for a combustion response of $\text{Re}(N) = 0$ and $\text{Im}(N) = -0.7$ a transverse wave of 0.9 the frequency of a pure acoustic wave exists. As the combustion response is increased the frequency increases and approaches the pure acoustic frequency when the combustion response is near the nozzle response; $\text{Re}(G) = 0.9166$ and $\text{IM}(G) = 0.0$. With the real part of the combustion response above the value for neutral stability the wave grows with time. A decrease in response results in a wave that decays. Decreasing the imaginary part of the combustion response from the neutral stability value results in a wave that grows with time. Decreasing the real part of the combustion response or increasing the imaginary part improves stability. To illustrate how various parameters influence the stability characteristics of a system, only the neutral stability line will be used.

Influence of Combustion Chamber Design on Neutral Stability

The influence of Mach number on neutral stability and wave profiles are shown in figs. 2 and 3. With low Mach numbers the stability line is almost vertical. The stability limit is therefore uniquely defined by the real portion of the combustion response. Frequencies with low Mach numbers are very close to those of a "pure" acoustic mode in a chamber with hard walls and ends. At very low Mach numbers the wave amplitude is constant with length and there is no phase displacement in the axial dimension.

At higher Mach numbers the neutral stability lines are generally rotated about the value of combustion response equal to the nozzle response. This rotation is accompanied by an increase in the variation of wave amplitude with length and phase shifting as shown in fig. 3. At low frequencies the amplitude at the nozzle end of the chamber leads the wave at the injector end (positive β angle). The amplitude variation lowers the real part of the combustion response needed to drive the wave.

At higher frequencies the opposite effects are observed. Amplitude is highest at the nozzle and the wave at the injector end leads the nozzle end. Generally it is found that when the real part of the combustion response is less than the real part of the nozzle response, the amplitude at the nozzle is less than at the injector. If the imaginary part of

the combustion response is less than the nozzle response the nozzle end of the wave leads the injector end.

Increasing the Mach number also increases the range of frequencies over which the system can oscillate. Within the limits of combustion response shown in fig. 2 a Mach number of 0.01 has a frequency variation of 0.1%, while a Mach number of 0.6 has a frequency variation of approximately 20%. Higher Mach numbers are also accompanied by several loops in the stability map as illustrated by the two loops shown for Mach number 0.6. These loops correspond to the first transverse mode combined with the various longitudinal modes. Each time the curve crosses itself it corresponds to going to one higher longitudinal mode in the combined mode. For a Mach number of 0.6 and at a reduced frequency $\omega/\omega_0 = 1.26$ the curve has crossed itself twice (two loops) and at this frequency the second longitudinal mode combined with the first transverse should be observed. The second mode is observed in fig. 3 for Mach number 0.6 and $\omega/\omega_0 = 1.26$ as there are two distinct minimums in the amplitude curve, corresponding to two pressure nodes. All the curves presented herein will form loops at higher frequencies.

The influence of chamber length to radius ratio (L/R) on the neutral stability lines and wave characteristics is shown in figs. 4 and 5. Decreasing the L/R generally moves the neutral stability line

down and to the right, thereby increasing the stable region of the system. Increasing the L/R produces more loops in the region where the combustion response is close to the nozzle impedance. Low L/R systems do not exhibit a significant phase shifting with length but do have appreciable amplitude variations as shown in fig. 5. The general characteristics of the influence of L/R are similar to those of Mach number as described previously.

The influence of nozzle flow response on neutral stability lines is shown in fig. 6. Reducing the real part of the nozzle response moves the curves to the left and decreases the stable region. Increasing the imaginary part of the response eliminates the loop and generally moves the curve down and to the right, thereby increasing the stable region. Improved stability is achieved by increasing the real and imaginary parts of the nozzle response.

Influence of Acoustic Liners

The influence of an acoustic liner is shown in fig. 7. Various liners are shown with three having the same absorption coefficient, α , which is generally used to characterize liners (ref. 1). For an absorption coefficient of 0.1 the three liners gave about the same results, lowering the curves and shifting them to the right, increasing the stable regime relative to the hard wall system. The greatest improvement occurs at higher frequencies. Further increasing the absorption coef-

ficient to 0.33 gave about three times the improvement achieved with a 0.1 coefficient.

Improvement in neutral stability lines with a 0.1 absorption coefficient liner for different L/R chambers is shown in fig. 8. Surprisingly, the L/R does not significantly change the effect of the liner even though more surface to volume is available to absorb the wave with large L/R 's. At large L/R the amplitude at the nozzle with a liner is much lower than without a liner. At small L/R the amplitude reduction is small. Thus, the increase in wall loss is compensated by a decrease in nozzle loss.

Improvement in neutral stability lines with a 0.1 absorption coefficient liner for different Mach numbers are shown in fig. 9. Mach number strongly controls the affect of an acoustic liner. At low Mach numbers the liner is extremely effective in increasing the stable regime. At higher Mach numbers the effectiveness of the liner is decreased. The large increase in effectiveness at low Mach numbers is again due to the change in amplitude at the nozzle. For low Mach numbers, the amplitude at the nozzle with a liner is greater than without a liner. Therefore the liner increased the loss through the nozzle as well as through the wall. At high Mach numbers, the liner decreases the nozzle end amplitude and losses.

Combining Combustion Process and System Responses

The previous sections have shown what combustion response is required at the injector end of a given combustor configuration to obtain various stability characteristics. The combustion process has a response which is determined by the injector, propellants, etc. A typical response for vaporization of liquid oxygen droplets is described in ref. 4 and shown in fig. 10. The vaporization response is determined by the dimensionless time $\omega\tau$ (ω is frequency of oscillation and τ is mean drop lifetime). At $\omega\tau = 0$ the real and imaginary parts of the vaporization response are zero. At infinite $\omega\tau$ the vaporization response goes to $\text{Re}(N) = -3.93$ and $\text{Im}(N) = 0.0$. Also shown in fig. 10 is the combustion response required for neutral stability for the reference combustor configuration described previously. System stability characteristics for the vaporization process with the reference combustor are obtained when the combustion response line intersects the vaporization response line at the same frequency. The lines intersect when $\omega\tau = 0.2$ and $\omega/\omega_0 = 0.98$ and when $\omega\tau = 2.2$ and $\omega/\omega_0 = 0.4$. Therefore, neutral stability would be obtained for $\tau = 0.2/\omega_0$ and $\tau = 5.5/\omega_0$. Between these τ values the system would be unstable as the vaporization response line would intersect combustion response lines of positive growth rates. Outside of these τ values the system would be stable as the intersection would be with

lines of negative growth rates. Neutral stability is obtained with a combustion response of $Re = 0.5$ and $Im = -0.03$ and with $Re = -2.25$ and $Im = -3.2$. These real values are much less than the 0.9166 values of the nozzle response. This illustrates why it is important to know the in-phase and out-of-phase portion of the combustion process response.

Studies with the reference combustor have shown that stability was very dependent on the hydrogen temperature or density (ref. 6). To explain this effect a model was postulated (ref. 5) in which stability was influenced by flow response of the gaseous hydrogen. The response of the hydrogen flow and oxygen vaporization process was obtained by a flow weighted average of the response of the oxidizer and the hydrogen, or

$$N = \frac{W_{OX}}{W_T} N_{OX} + \frac{W_f}{W_T} N_f \quad (17)$$

Curves of hydrogen response (N_f) were calculated for different hydrogen densities. Results of these calculations for the "Reference 1" system of ref. 5 are shown in fig. 11. Response of the L_{OX} is $Re(N) = 0.56$ and $Im(N) = -0.02$ obtained from fig. 11 at an $\omega \tau = 0.2$. The combustion response curve crosses the combined hydrogen flow and L_{OX} vaporization response line at a hydrogen density of 0.48 which is within the 0.4 to 0.5 density limits obtained experimentally (fig. 5 of ref. 5).

Studies with the same combustion chamber showed (ref. 1, figs. 29 and 30) that an acoustic liner with an absorption coefficient of 0.08 reduced the hydrogen temperature from 110° R with no liner to between 95° and 60° R with the liner. This corresponds to a hydrogen density increase from 0.48 to between 0.59 and 0.98. The combined hydrogen and oxygen response curve of fig. 11 intersect the 0.1 absorption coefficient liner calculations at a density of 0.90, which is in reasonable agreement with experiment. Better agreement would have been obtained if a larger $\omega\tau$ had been assumed for the oxidizer. This also shows the importance of the imaginary part of the combustion response. Increasing the $\omega\tau$ of the oxidizer mainly lowers the combined hydrogen and oxygen response curve of fig. 11. Since without a liner the combustion response is almost vertical at the point of intersection a small change in $\omega\tau$ of the L_{OX} would not influence the stability limits. With a liner added the influence would be very significant as the liner curve is not vertical.

CONCLUSIONS

A mathematical model to determine stability characteristics of rocket combustors with high Mach number flow and acoustic liners has been presented. Calculations performed with this model for the first transverse mode have shown many characteristics observed in actual combustors.

1. Variation in wave amplitude with axial position
2. Phase or time displacement of the wave with length
3. Strong influence of Mach number and length to radius ratio on stability limits
4. Range of possible frequencies of oscillations with a given combustor configuration

With this model it is possible to determine what acoustic liner is required to stabilize a combustor. Calculations have illustrated the importance of the perturbation in burning that occurs out of phase (90°) with the pressure oscillations.

NOMENCLATURE

A	cross sectional area of combustor
a	speed of sound
B_1, B_2	complex coefficients given by eq. (6)
C	complex coefficient given by eq. (13)
D	total derivative
e	exponential
G	complex number specifying nozzle response eq. (11)
g	gravitational constant
$\text{Im}(\)$	imaginary part of term in ()
i	unit complex = $\sqrt{-1}$
J_n	Bessel function of Order n

K	velocity response at chamber walls, eq. (12) or (15)
L	length of chamber
M	Mach number
m	argument of bessel function
N	combustion response eq. (11) or (14)
n	number of pressure modes in θ direction
P	pressure
P_{\max}	amplitude of pressure oscillations
Q	constant of integration from integrating the momentum equation = $1 + \frac{\gamma - 1}{2} M^2$
Re()	real part of ()
r	radial dimension
T	temperature
t	time
u	velocity vector
v_{θ}	velocity in tangential
v_r	velocity in radial direction
v_z	velocity in axial direction
W	flow rate
Z	axial direction

α	absorption coefficient = $\frac{4\text{Re}(K)}{[\text{Re}(K) + 1]^2 + [\text{Im}(k)]^2}$
β	angular position of maximum amplitude
γ	specific heat ratio
ϵ	perturbation amplitude
θ	tangential direction
ρ	density
τ	average vaporization time
Φ	velocity potential $\nabla(\Phi) = u$
ω	frequency of oscillation
ω_0	frequency of oscillation = $a \times 0.586/2R$
∇	del operator

Subscripts:

f	fuel
ox	oxidizer
t	derivative with respect to time

Superscripts:

(1)	perturbation quantity to order (1) of perturbation amplitude ()
-	time average value

REFERENCES

1. Wanhainen, J. P., Bloomer, H. E., Vincent, D. V., and Curley, J. K.: Experimental Investigation of Acoustic Liners to Suppress Screech in Hydrogen-Oxygen Rockets, NASA TN D-3822, 1967.
2. Clayton, R. M. and Ragero, R. S.: Experimental Measurements on A Rotating Detonation-Like Wave Observed During Liquid Rocket Combustion, California Institute of Technology, Jet Propulsion Laboratory Technical Report 32-788, August 1965.
3. Maslen, S. and Moore, F. K.: J. Aeron. Sci. 23, 583 (1956).
4. Heidmann, M. F. and Wieber, P. R.: Analysis of Frequency Response Characteristics of Propellant Vaporization, NASA TN D-3749, 1966.
5. Feiler, C. E. and Heidmann, M. F.: Dynamic Response of Gaseous-Hydrogen Flow System and its Application to High Frequency Combustion Instability, NASA TN D-4040, 1967.
6. Wanhainen, J. P., Parish, H. C., and Conrad, E. W.: Effect of Propellant Injection Velocity on Screech in a 20 000-Pound Hydrogen-Oxygen Rocket Engine, NASA TN D-3373, 1966.
7. Kesselring, R. C. and Obert, C. L.: Combustion Instability of Metallized Gelled Propellants, Rocketdyne Division, North American Aviation, Inc. (AFRPL-TR-67-164, DDC No. AD-816987), May 1967.

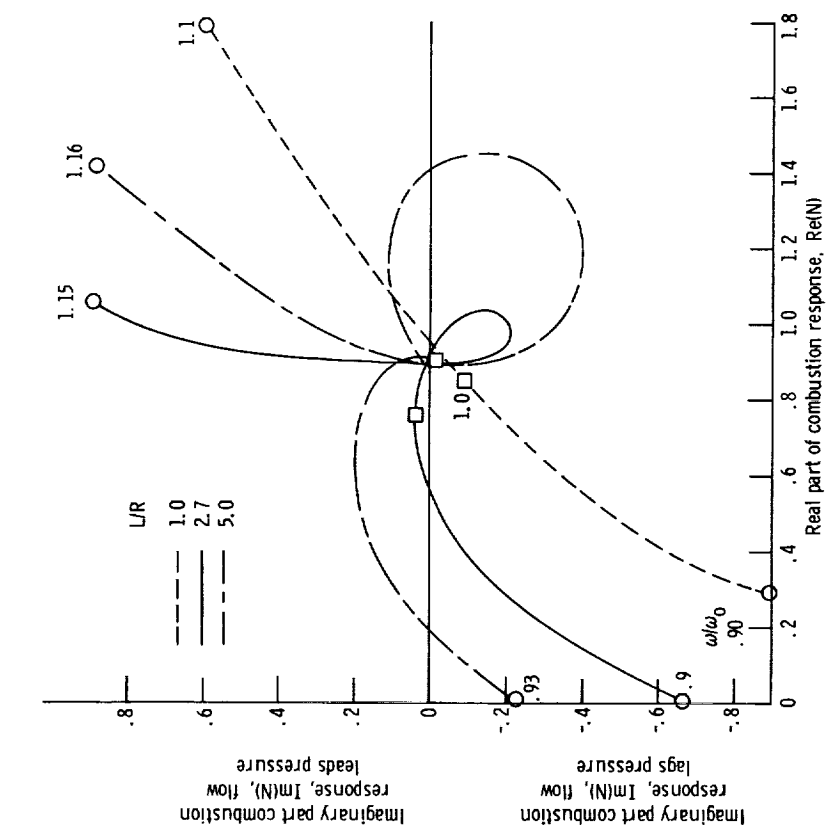


Figure 4. - Influence of chamber length to radius ratio on neutral stability limits. Mach number, 0.33; nozzle response, $Re(G) = 0.9166$, $Im = 0$, hard wall chamber.

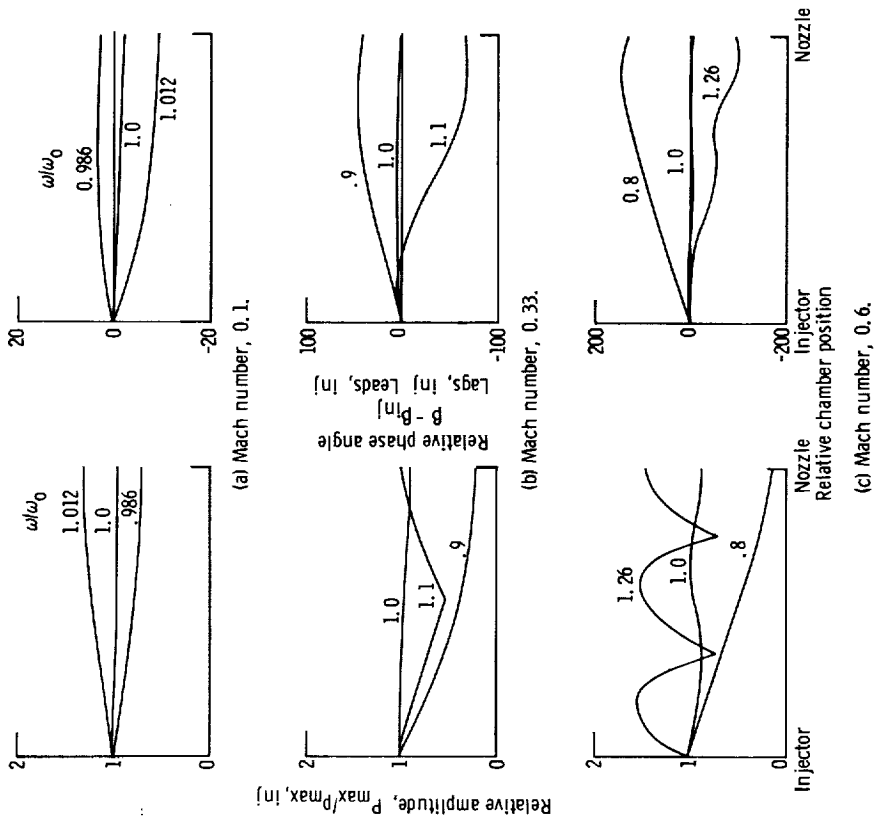


Figure 3. - Pressure profiles with various Mach numbers and frequencies. Chamber length/radius, 2.7; nozzle coefficient, $Re(G) = 0.9166$, $Im(G) = 0$, hard wall chamber.

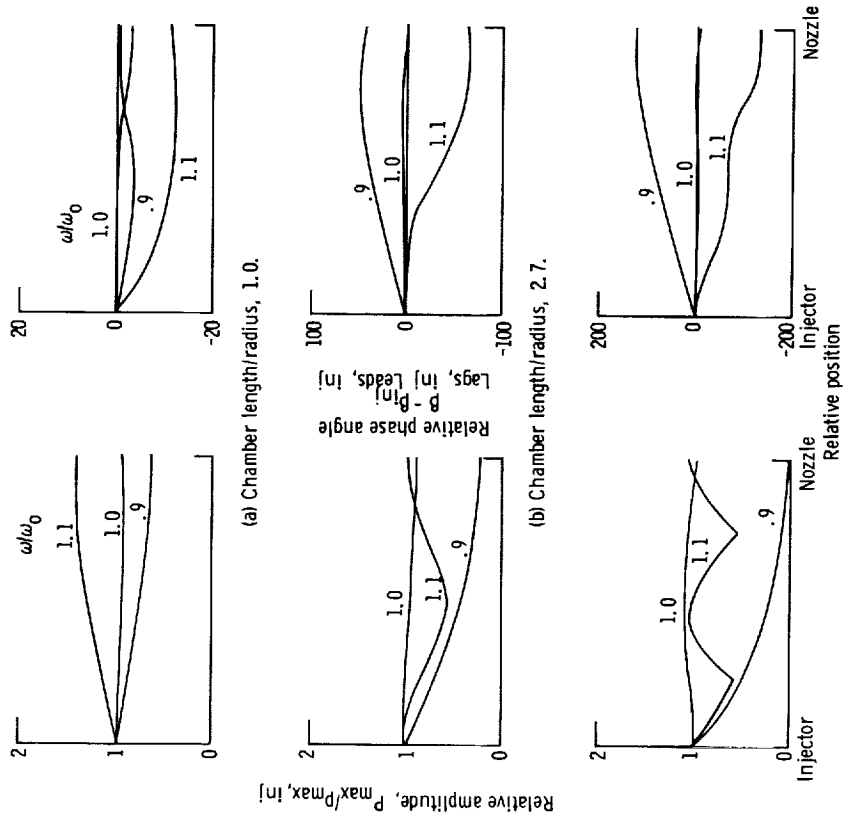


Figure 5. - Pressure profiles with various length to radius ratio and frequencies. Mach number, 0.33; nozzle response, $RE(G) = 0.9166$, $IM(G) = 0$, hard walls.

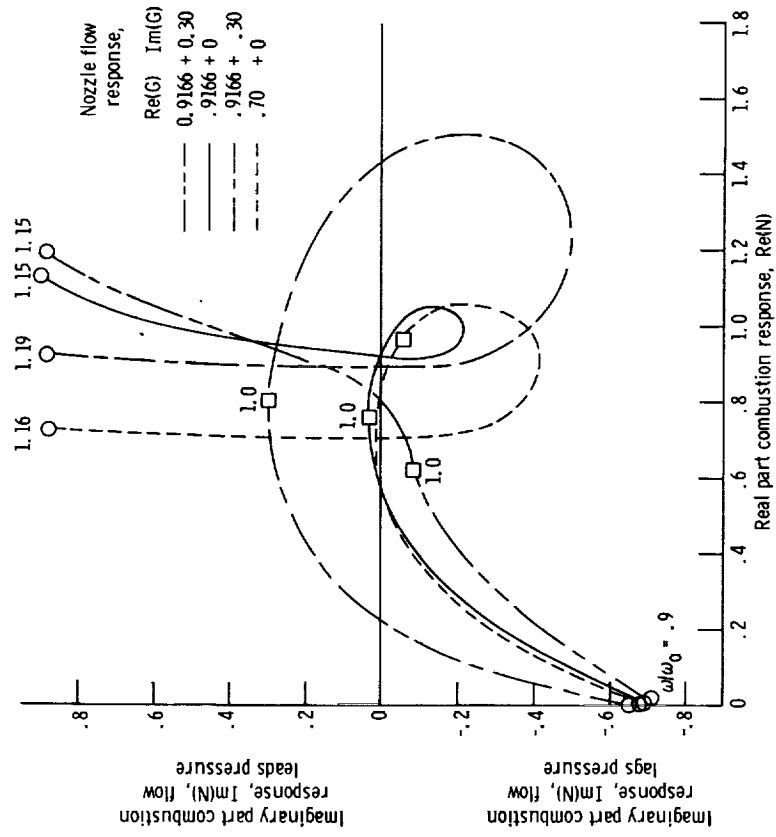


Figure 6. - Influence of nozzle flow response on neutral stability limits. Chamber length/radius, 2.7; Mach number flow, 0.33, hard wall chamber.

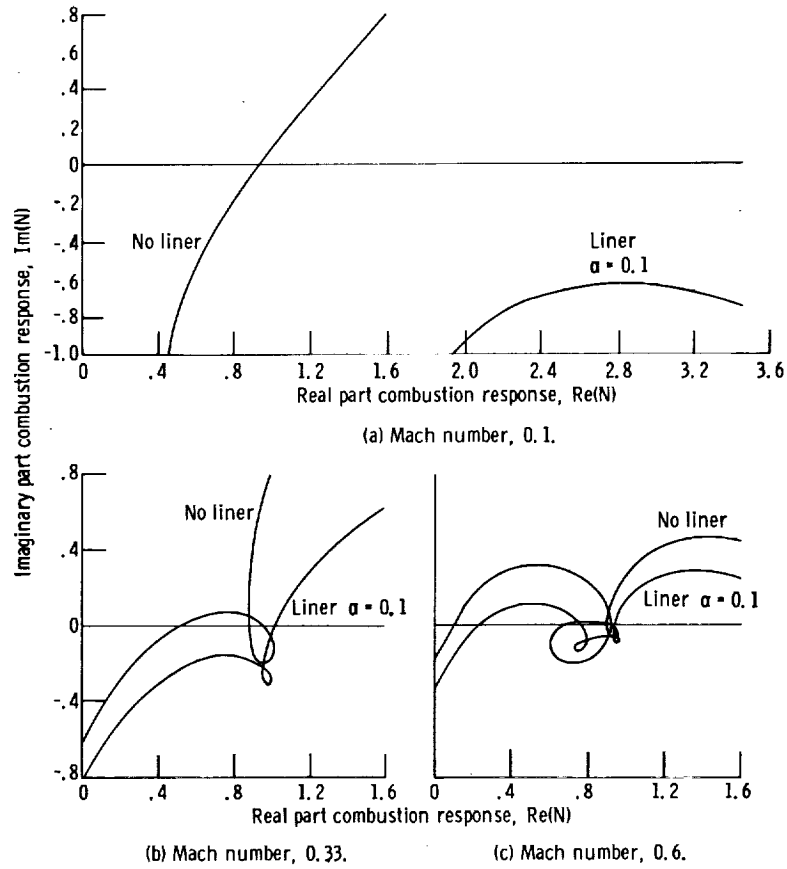


Figure 9. - Influence of an acoustic liner on stability limits with different Mach numbers. Length to radius ratio, 2.7. Nozzle response, $Re(G) = 0.9166$, $Im(G) = 0$.

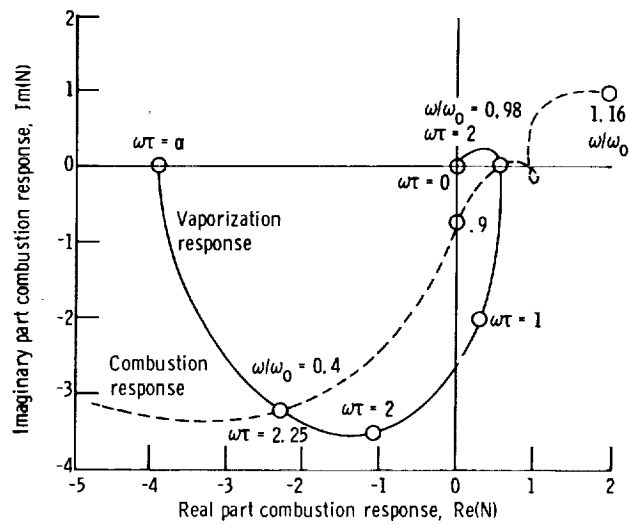


Figure 10. - Combined response curves of oxygen vaporization with reference combustion chamber. Mach number, 0.33, nozzle coefficient, $Re(G) = 0.9166$, $Im(G)$, hard wall.

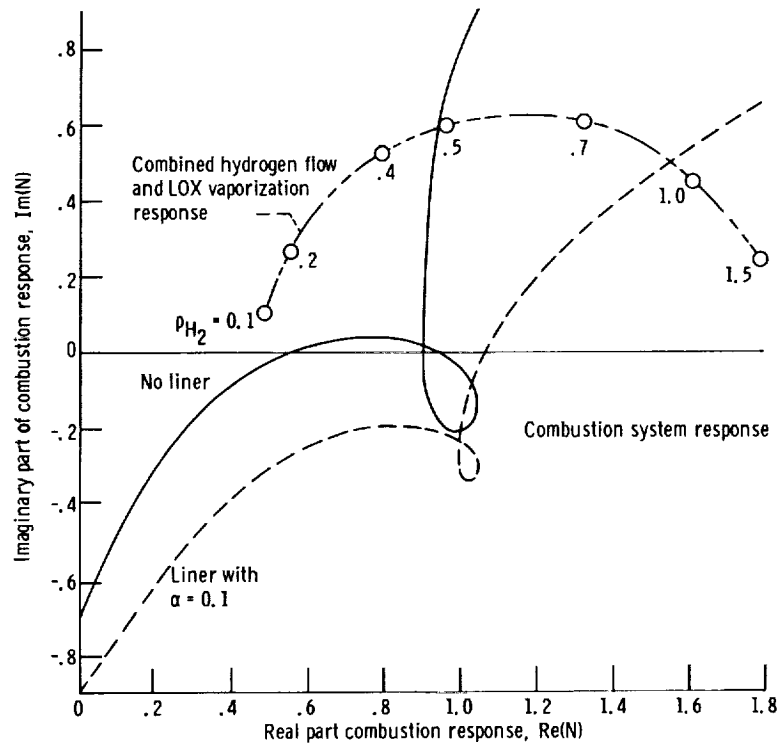


Figure 11. - Combined combustion system response curves with hydrogen flow and LOX vaporization response. Mach number, 0.33; length to radius ratio, 2.7; nozzle response, $Re(G)$, 0.9166, $Im(G) = 0$.